Catalytic Hydroetherification of Unactivated Alkenes Enabled by Proton-Coupled Electron Transfer

Elaine Tsui, Anthony J. Metrano, Yuto Tsuchiya, and Robert R. Knowles*

Department of Chemistry, Princeton University, Princeton, New Jersey 08544, United States

Supporting Information Placeholder

ABSTRACT: We report a light-driven, catalytic protocol for the intramolecular hydroetherification of unactivated alkenols to furnish cyclic ether products. These reactions occur under visible light irradiation in the presence of an Ir(III)-based photosensitizer, a Brønsted base catalyst, and a hydrogen atom transfer co-catalyst. Reactive alkoxy radicals are proposed as key intermediates that are generated by direct homolytic activation of alcohol O–H bonds through a proton-coupled electron transfer mechanism. This method exhibits a broad substrate scope and high functional group tolerance, and it accommodates a diverse range of alkene substitution patterns. Results demonstrating the extension of this catalytic system to carboetherification reactions are also presented.

The addition of alcohols to alkenes is a powerful approach to C–O bond formation and the construction of oxygen heterocycles. Accordingly, numerous olefin hydroetherification methods have been developed using Brønsted acid- or transition metal-based catalysts (**Figure 1a**), which typically operate through either electrophilic alkene activation or migratory insertion mechanisms.[1–5] While elegant and effective, these reactions are often sensitive to C=C substitution patterns and typically afford Markovnikov-type addition products. More recently, Nicewicz and co-workers demonstrated an alternative mode of alkene activation, wherein single-electron oxidation of an olefin by an excited-state redox catalyst furnishes an electrophilic alkene radical cation that can be subsequently trapped by an alcohol nucleophile.[6] While this method affords complementary anti-Markovnikov regioselectivity, its use is currently limited to oxidizable styrenyl and trisubstituted alkyl olefin substrates. Considering these strategies more broadly, the development of a general catalytic protocol for intramolecular hydroetherification that accommodates electronically unbiased alkenes with variable substitution remains an outstanding challenge.

In contrast to these alkene activation strategies, we recently became interested in an orthogonal approach to olefin hydroetherification involving direct homolytic activation of alcohol O–H bonds to furnish reactive alkoxy radical intermediates (**Figure 1b**). Electrophilic alkoxy radicals are well known to undergo addition to pendent alkenes to generate cyclic ethers with predictable 5-*exo-trig* regioselectivity.[7–9] While these seminal studies have firmly established the feasibility of radical C–O bond formation, effective generation of the requisite *O*-centered radicals typically requires either prefunctionalization of the hydroxyl group or the use of stoichiometric reagents and harsh reaction conditions. Therefore, the development of a mild, catalytic protocol for olefin hydroetherification utilizing alkoxy radicals derived from simple alcohol starting materials has the potential to advance the value of radical-based etherification in synthesis.

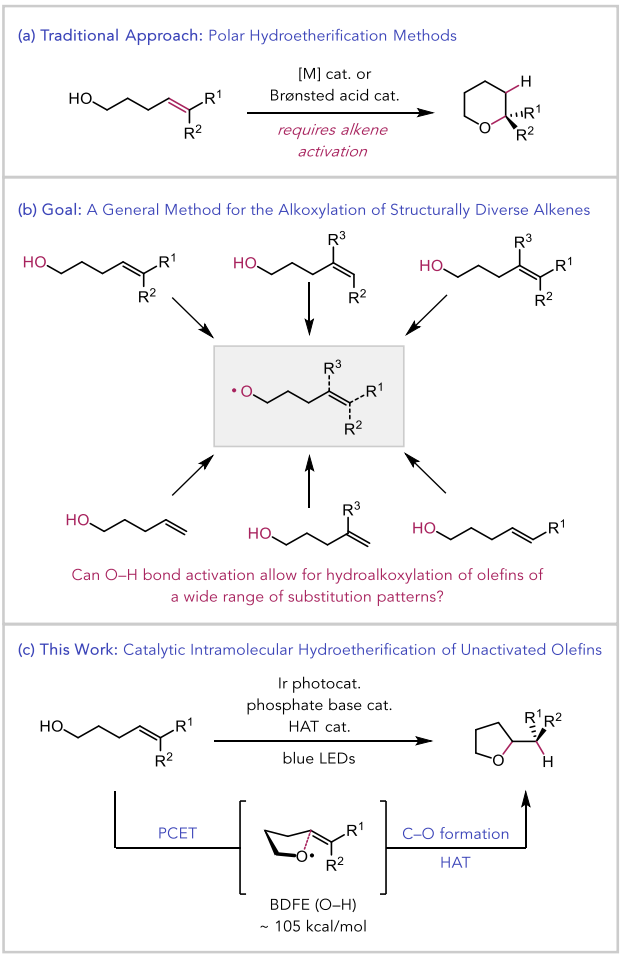

Figure 1. (a) Traditional approaches to hydroetherification involving alkene activation. **(b)** Development of a general strategy for hydroalkoxylation *via* O–H activation. **(c)** PCET-mediated hydroetherification of unactivated alkenes.

To this end, our group has recently developed excited-state proton-coupled electron transfer (PCET) methods for the direct homolytic activation of alcohol O–H bonds to access alkoxy radical intermediates.[10,11] While our prior work focused on alkoxy radical-mediated C–C bond β-scission reactions, we questioned whether similar reactivity could be adapted for use in olefin

hydroetherification reactions to generate cyclic ethers directly from readily accessible alkenols (**Figure 1c**). We envisioned a prospective catalytic cycle for this transformation wherein PCET activation of the alcohol O–H bond of the substrate would form a reactive alkoxy radical intermediate through the concerted action of an Ir(III)-based visible-light photooxidant and a weak Brønsted base catalyst (**Figure 2**).[12] The resulting *O*-centered radical would undergo addition to a pendent olefin, forming a new C–O bond and an adjacent alkyl radical. Hydrogen-atom transfer (HAT) from a thiol-derived co-catalyst to the *C*-centered radical would furnish the desired cyclic ether.[13] Subsequent reduction of the thiyl radical by the Ir(II) state of the photocatalyst and protonation of the resulting thiolate by the conjugate acid of the Brønsted base would close the catalytic cycle.

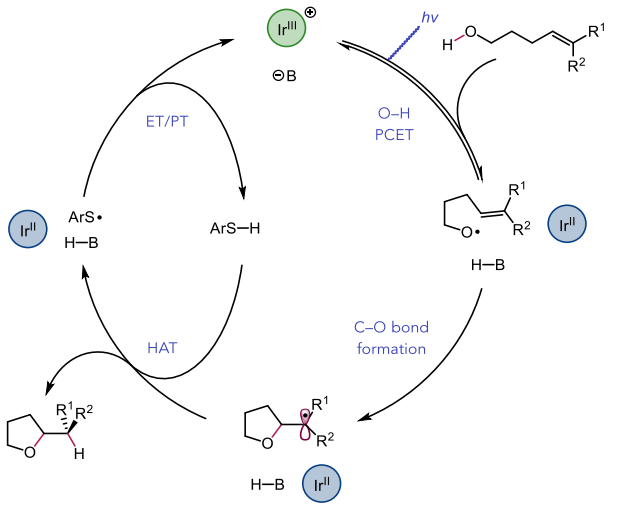

Figure 2. Prospective catalytic cycle.

Our optimization studies focused on 1,2-disubstituted alkenol substrate **1** (**Table 1**). Adapting conditions from our prior work in N–H[14] and O–H[10] PCET reactions, we found that 2 mol% of [Ir(dF(CF$_3$)ppy)$_2$(5,5′-d(CF$_3$)bpy)]PF$_6$ photocatalyst, 20 mol% of diphenyl phosphate base, and 20 mol% of 2,4,6-triisopropylthiophenol (TRIP-SH) in trifluorotoluene solvent under blue light irradiation (~ 450 nm) afforded the desired ether product **2** in 31% yield (entry 1). Notably, this highly oxidizing photocatalyst ($E^{III*/II}$ = +1.30 V vs. Fc$^+$/Fc in MeCN)[15] is required—in combination with phosphate bases (pK_a ~ 13 in MeCN)[16]—to achieve effective bond dissociation free energies (BDFEs) approaching that of the alcohol O–H bond (BDFE ~ 105 kcal/mol).[12b] Less oxidizing Ir(III)-based photocatalysts were ineffective in the reaction, providing no yield of **2** (see Supporting Information, Table S1). The counter-cation of the phosphate base was found to have a marked effect on the reaction efficiency, as the tetrabutylphosphonium ion led to a 40% boost in yield compared to the corresponding ammonium cation (entry 2). This effect is possibly due to the enhanced solubility of tetrabutylphosphonium diphenyl phosphate in trifluorotoluene or perhaps to the more dissociated nature of the ion pair.[17] The use of either dialkyl phosphates or trifluoroacetate did not improve the yields further (entries 3–5). We next turned our attention toward the optimization of the HAT co-catalyst by examining a series of electron-rich and electron-deficient thiophenols (entries 6–11). Interestingly, 2-fluorothiophenol outperformed the other thiols examined, providing **2** in 75% yield (entry 10)—a notable improvement over the other fluorothiophenol regioisomers (entries 8–9). The corresponding disulfide was equally effective in the reaction (entry 12), and we therefore elected to use 1,2-bis(2-fluorophenyl)disulfide as the HAT co-catalyst due to its ease of handling.[6b]

Table 1. Reaction Optimization[a]

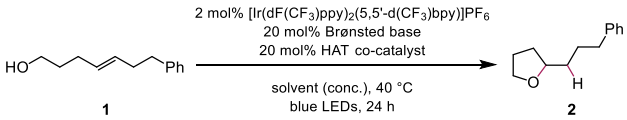

Entry	Brønsted Base	HAT Co-Catalyst	Solvent (Conc., M)	GC Yield[b]
1	Bu_4N^+ $(PhO)_2P(O)O^-$	TRIP-SH	$PhCF_3$ (0.1)	31%
2	Bu_4P^+ $(PhO)_2P(O)O^-$	TRIP-SH	$PhCF_3$ (0.1)	71%
3	Bu_4P^+ $(n\text{-}BuO)_2P(O)O^-$	TRIP-SH	$PhCF_3$ (0.1)	48%
4	Bu_4P^+ $(t\text{-}BuO)_2P(O)O^-$	TRIP-SH	$PhCF_3$ (0.1)	33%
5	Bu_4P^+ $CF_3C(O)O^-$	TRIP-SH	$PhCF_3$ (0.1)	54%
6	Bu_4P^+ $(PhO)_2P(O)O^-$	Ph-SH	$PhCF_3$ (0.1)	45%
7	Bu_4P^+ $(PhO)_2P(O)O^-$	4-(MeO)PhSH	$PhCF_3$ (0.1)	41%
8	Bu_4P^+ $(PhO)_2P(O)O^-$	4-FPhSH	$PhCF_3$ (0.1)	59%
9	Bu_4P^+ $(PhO)_2P(O)O^-$	3-FPhSH	$PhCF_3$ (0.1)	47%
10	Bu_4P^+ $(PhO)_2P(O)O^-$	2-FPhSH	$PhCF_3$ (0.1)	75%
11	Bu_4P^+ $(PhO)_2P(O)O^-$	4-(CF_3)PhSH	$PhCF_3$ (0.1)	45%
12	Bu_4P^+ $(PhO)_2P(O)O^-$	$(2\text{-FPhS})_2$	$PhCF_3$ (0.1)	74%
13	Bu_4P^+ $(PhO)_2P(O)O^-$	$(2\text{-FPhS})_2$	PhMe (0.1)	58%
14	Bu_4P^+ $(PhO)_2P(O)O^-$	$(2\text{-FPhS})_2$	CH_2Cl_2 (0.1)	49%
15	Bu_4P^+ $(PhO)_2P(O)O^-$	$(2\text{-FPhS})_2$	1,4-dioxane (0.1)	20%
16	Bu_4P^+ $(PhO)_2P(O)O^-$	$(2\text{-FPhS})_2$	$PhCF_3$ (0.05)	80%

Entry	Change from Entry 16	GC Yield[b]
17	30 mol% $(2\text{-FPhS})_2$	85%
18	no light	0%
19	no Ir(III) photocatalyst	0%
20	no Brønsted base	11%
21	no HAT co-catalyst	9%

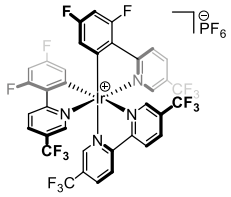

Photocatalyst
[Ir(dF(CF$_3$)ppy)$_2$(5,5′-d(CF$_3$)bpy)]PF$_6$

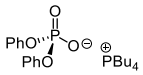

Brønsted Base
Bu_4P^+ $(PhO)_2P(O)O^-$

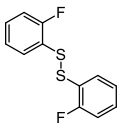

HAT Co-Catalyst
$(2\text{-FPhS})_2$

[a]Reactions were run on a 0.05 mmol scale. [b]GC yields determined relative to biphenyl as an internal standard.

Various other solvents proved to be less effective in the reaction (entries 13–15), but decreasing the reaction concentration increased the yield to 80% (entry 16). By adjusting the HAT co-catalyst loading to 30 mol%, tetrahydrofuran **2** was obtained in 85% yield, providing our optimal reaction conditions (entry 17). Control experiments run in the absence of light and photocatalyst furnished no product, and significantly reduced yields were observed in the absence of Brønsted base and HAT co-catalyst (entries 18–21). For more easily oxidizable alkenes, such as trisubstituted and styrenyl olefins, diminished conversion to the desired ether products was observed, suggesting that an alternative but much less efficient alkene oxidation pathway could also be operative.[6] This observation, however, does not preclude the viability of a dominant alkoxy radical-mediated mechanism under the optimal PCET conditions (*vide infra*).

Table 2. Substrate Scope[a]

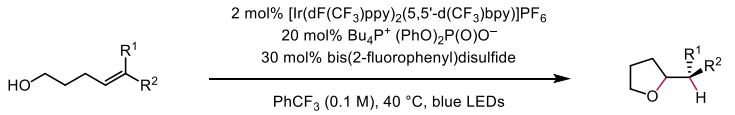

Disubstituted Alkenes

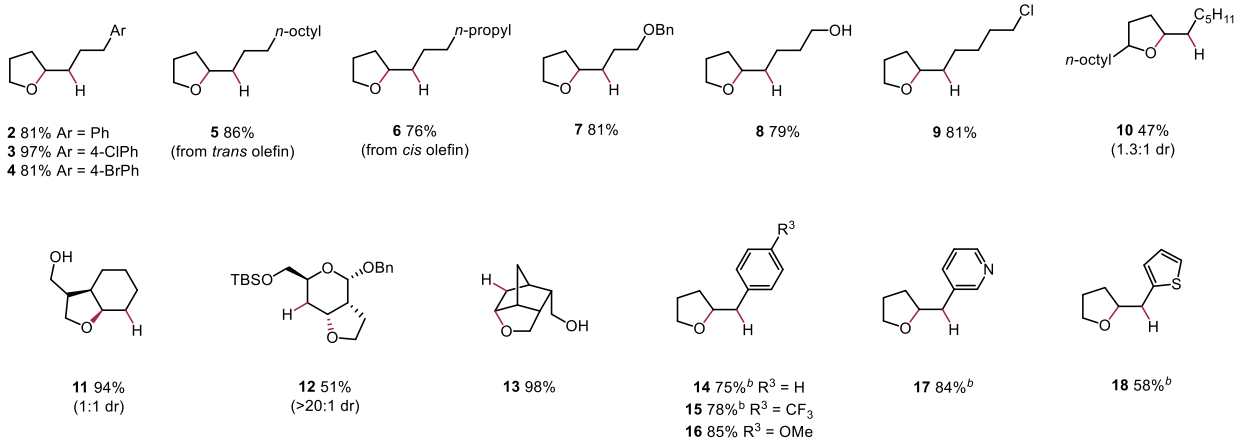

2 81% Ar = Ph
3 97% Ar = 4-ClPh
4 81% Ar = 4-BrPh

5 86%
(from *trans* olefin)

6 76%
(from *cis* olefin)

7 81%

8 79%

9 81%

10 47%
(1.3:1 dr)

11 94%
(1:1 dr)

12 51%
(>20:1 dr)

13 98%

14 75%[b] R^3 = H
15 78%[b] R^3 = CF_3
16 85% R^3 = OMe

17 84%[b]

18 58%[b]

Trisubstituted Alkenes

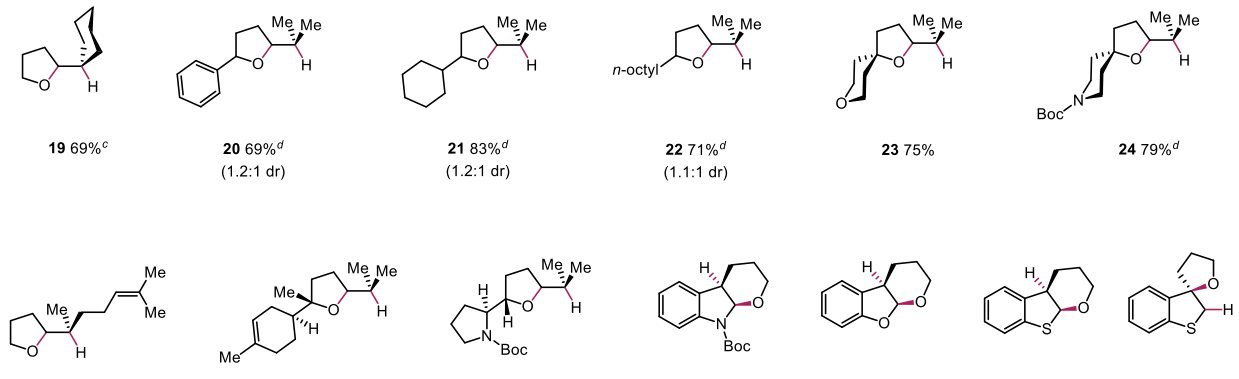

19 69%[c]

20 69%[d]
(1.2:1 dr)

21 83%[d]
(1.2:1 dr)

22 71%[d]
(1.1:1 dr)

23 75%

24 79%[d]

25 70%[b]
(1:1 dr)

26 78%[d]
(1.1:1 dr)

27 from *syn* 78%[d] (2:1 dr)
28 from *anti* 78%[d] (1.3:1 dr)

29 90%[d]
(>20:1 dr)

30 70%[d]
(>20:1 dr)

31 85%[d], 2.5:1 *endo*/*exo* (**31a**:**31b**)
(for **31a**, >20:1 dr)

Monosubstituted Alkenes

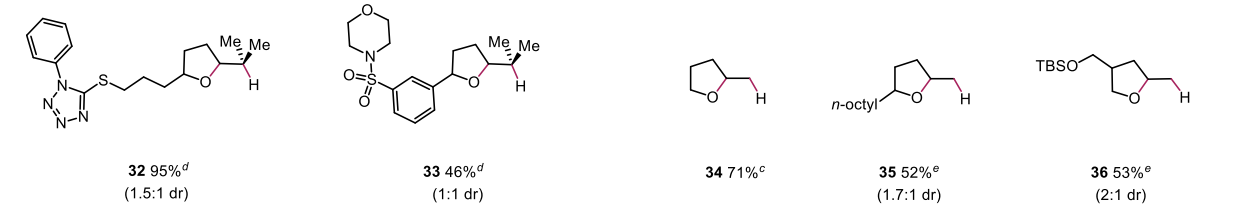

32 95%[d]
(1.5:1 dr)

33 46%[d]
(1:1 dr)

34 71%[c]

35 52%[e]
(1.7:1 dr)

36 53%[e]
(2:1 dr)

[a]Reactions were performed on a 0.5 mmol scale. Reported yields are for isolated and purified material unless otherwise noted and represent the average of two experiments. [b]Bu_4N^+ $CF_3C(O)O^-$ used as the base. [c]GC yield is reported relative to an internal standard due to volatility. [d]2-methyl-2-oxazoline used as the base, and 4-trifluoromethylthiophenol used as the HAT co-catalyst. [e]1,2-Bis(4-methoxyphenyl)disulfide used as the HAT co-catalyst.

Interestingly, different classes of alkenols with respect to the olefin substitution pattern perform optimally when tailored catalyst combinations are used. The highest yields for terminal olefins are obtained when 1,2-bis(4-methoxyphenyl)disulfide, a more electron-rich HAT co-catalyst, is employed, while trisubstituted olefins prefer heterocyclic bases, such as 2-methyl-2-oxazoline, and electron-deficient thiols, such as 4-trifluoromethylthiophenol (see Supporting Information, Tables S2 & S3). While our general optimization parameters are applicable to a broad scope of substrates, these substrate-specific conditions provide a meaningful improvement in yield.

Having established the optimized reaction conditions, we next examined the scope of this reaction with respect to various alkene substitution patterns (**Table 2**). With the success of model substrate **1**, we also found that a range of other 1,2-disubstituted olefins gave excellent yields of the desired cyclic ether products (**3**–**9**). Both *cis* and *trans* olefins participated in the reaction with comparable efficiencies (**5**, **6**), and the presence of various functional groups, such as benzyl ethers, free alcohols, and alkyl halides, were well tolerated under the reaction conditions (**7**–**9**). Hydroetherification of disubstituted olefins with secondary alcohols also proved to be viable, albeit with moderate reactivity (**10**). Notably, this protocol provides direct access to a variety of bicyclic structures from alcohol precursors, forming fused rings (**11**), including glucal derivatives (**12**), and bridged ethers (**13**) with high diastereoselectivity. In addition to aliphatic 1,2-disubstituted olefins, electronically diverse styrenyl alkenes were competent substrates (**14**–**16**), and pyridine and thiophene derivatives furnished tetrahydrofuran products (**17**, **18**) in good yields.

With respect to trisubstituted alkenes, anti-Markovnikov hydroetherification proceeded with primary, secondary, and tertiary alcohols (**19**–**24**), providing ether products that are generally not accessible using traditional hydroalkoxylation strategies. Interestingly, products resulting from competing C–C β-scission were not observed during the formation of **23** and **24**, enabling facile and efficient synthesis of spirocyclic scaffolds. Derivatives of terpenoids, such as linalool and bisabolol, were also obtained in good yields using this protocol (**25**, **26**), leaving the more distal olefins unaffected and demonstrating that 5-*exo*-*trig* cyclization is preferred.

We also evaluated the cyclization reactions of two diastereomers of an *N*-Boc-L-prolinol derivative and found that both *syn* and *anti* alkenols were transformed to their respective tetrahydrofuran products in good yields (**27**, **28**). Of particular note is that the remaining mass balance in these reactions was predominantly comprised of the β-scission product, *N*-Boc-pyrrolidine. This observation serves as evidence that a discrete alkoxy radical intermediate is formed under these PCET conditions and is consistent with an alkoxy radical-mediated mechanism for C–O bond formation. Moreover, the high yield of cyclized product suggests that these electrophilic *O*-centered radicals react more rapidly with electron-rich alkenes than they undergo C–C cleavage, even when the *C*-centered radical resulting from β-scission is stabilized by an adjacent heteroatom.[10c] In contrast, when the monosubstituted and 1,2-disubstituted variants of this substrate were studied under the reaction conditions, only *N*-Boc-pyrrolidine was formed (see Supporting Information, Table S6), consistent with a kinetically less favorable C–O bond-forming event.

Interestingly, *N*-Boc-indole and benzofuran derivatives proceeded through 6-*endo*-*trig* cyclizations to favor generation of an intermediate tertiary benzylic radical, affording tricyclic ether products in excellent yields and diastereoselectivities (**29**, **30**). In the case of benzothiophene, a 2.5:1 ratio of 6-*endo* and 5-*exo* products was formed, allowing access to both fused- and spiro-cyclic structures (**31a**, **31b**). Moreover, this hydroetherification protocol can tolerate the presence of polar functionality, operating in systems containing *N*-phenyltetrazole thioethers and sulfonamides (**32**, **33**). Remarkably, hydroalkoxylation of unactivated monosubstituted alkenes can also be achieved in moderate to good yields, even with generation of a primary *C*-centered radical after cyclization (**34**–**36**).

Lastly, we evaluated the synthetic versatility of our hydroalkoxylation protocol in the context of olefin carboetherification reactions,[18] wherein electron-deficient olefins were used to intercept the intermediate *C*-centered radical following C–O bond formation. When 4-cyclohexylidenebutan-1-ol was subjected to reaction conditions in which the HAT co-catalyst is replaced with a stoichiometric acceptor olefin, a range of alkylated ethers were furnished with good efficiency (**Table 3**). Specifically, tetrahydrofuran derivatives were successfully alkylated with α-phenyl methacrylate (**37**), dimethyl fumarate (**38**), and dehydroalanine derivative (**39**), demonstrating that intermolecular C–C bond formation can be achieved following alkoxy radical cyclization. Moreover, acceptors containing heterocyclic scaffolds, such as 2-vinylpyridine (**40**) and 2-vinylpyrazine (**41**), provided modest yields of alkylated product. Even in cases where a primary alkyl radical is generated upon cyclization, addition to α-phenyl methacrylate outcompetes other possible reaction pathways to give the desired difunctionalization product (**42**). Carboetherification of a secondary alkenol with 1,1-bis(phenylsulfonyl)ethylene also proceeded in good yield (**43**). These results highlight the potential for alkoxy radical-mediated C–O bond formation to be adapted for further product derivatization.

Table 3. Carboetherification of Unactivated Alkenes[a]

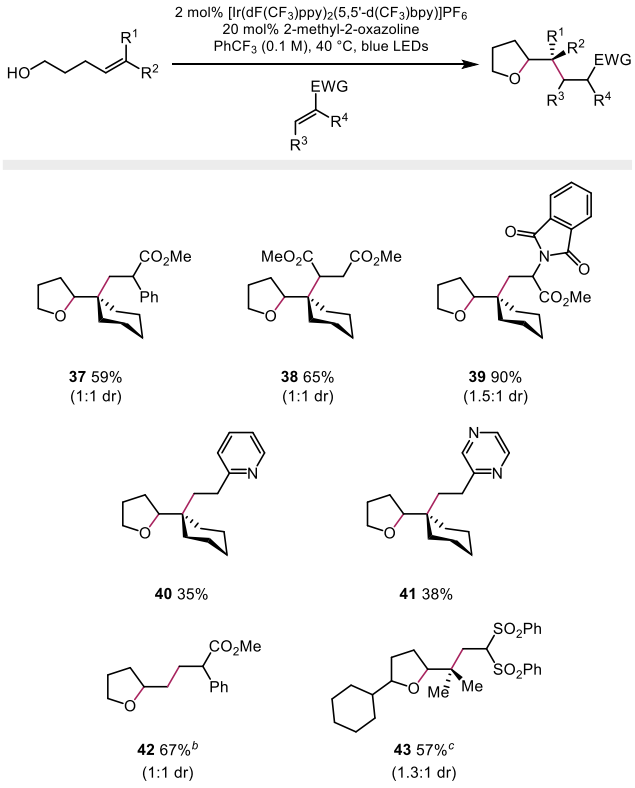

[a]Reactions were performed on a 0.5 mmol scale. Reported yields are for isolated and purified material unless otherwise noted and represent the average of two experiments. [b]Bu_4P^+ $(PhO)_2P(O)O^-$ used as the base. [c]Reactions were performed on a 0.25 mmol scale in $PhCF_3$ (0.05 M).

In summary, we have developed a catalytic protocol for the intramolecular hydroetherification of unactivated alkenes with a wide range of substitution patterns. This work leverages light-driven PCET for the direct homolysis of strong alcohol O–H bonds, enabling the activation of common hydroxyl groups, which stands in contrast to traditional approaches that require alkene activation or alcohol prefunctionalization. Taken together, this strategy further illustrates the potential of excited-state PCET to access alkoxy radicals from simple alcohol starting materials under mild, catalytic conditions.

ASSOCIATED CONTENT

Supporting Information

The Supporting Information is available free of charge on the ACS Publications website.

Experimental procedures, additional optimization data, characterization data for all new compounds, and spectral data (PDF).

AUTHOR INFORMATION

Corresponding Author

*rknowles@princeton.edu

ORCID

Elaine Tsui: 0000-0002-5872-4824
Anthony J. Metrano: 0000-0002-2599-8917
Robert R. Knowles: 0000-0003-1044-4900

Notes

The authors declare no competing financial interests.

ACKNOWLEDGMENTS

Financial support was provided by the NIH (R35 GM134893). A.J.M. is grateful to the National Institute of General Medical Sciences of the NIH for a postdoctoral fellowship (F32 GM128245). Y.T. thanks the Institute of Transformative Bio-Molecules (WPI-ITbM), Nagoya University for support. The authors would like to thank Alec Mendelsohn for the synthesis of materials and helpful discussions. We also acknowledge Nick Chiappini and Hunter Ripberger for the preparation of materials.

REFERENCES

(1) For selected reviews and discussions of transition metal- and Brønsted acid-catalyzed hydroetherification, see: (a) Hintermann, L. Recent Developments in Metal-Catalyzed Additions of Oxygen Nucleophiles to Alkenes and Alkynes. *Top. Organomet. Chem.* **2010**, *31*, 123–155. (b) Beller, M.; Seayad, J.; Tillack, A.; Jiao, H. Catalytic Markovnikov and Anti-Markovnikov Functionalization of Alkenes and Alkynes: Recent Developments and Trends. *Angew. Chem. Int. Ed.* **2004**, *43*, 3368–3398. (c) Zeng, X. Recent Advances in Catalytic Sequential Reactions Involving Hydroelement Addition to Carbon-Carbon Multiple Bonds. *Chem. Rev.* **2013**, *113*, 6864–6900. (d) Rosenfeld, D. C.; Shekhar, S.; Takemiya, A.; Utsunomiya, M.; Hartwig, J. F. Hydroamination and Hydroalkoxylation Catalyzed by Triflic Acid. Parallels to Reactions Initiated with Metal Triflates. *Org. Lett.* **2006**, *8*, 4179–4182.

(2) For selected examples of hydroetherification of activated alkenes, see: (a) Nising, C. F.; Bräse, S. The Oxa-Michael Reaction: From Recent Developments to Applications in Natural Product Synthesis. *Chem. Soc. Rev.* **2008**, 1218–1228. (b) Zhang, Z.; Widenhoefer, R. A. Gold(I)-Catalyzed Intramolecular Enantioselective Hydroalkoxylation of Allenes. *Angew. Chem. Int. Ed.* **2007**, *46*, 283–285. (c) Hamilton, G. L.; Kang, E. J.; Mba, M.; Toste, F. D. A Powerful Chiral Counterion Strategy for Asymmetric Transition Metal Catalysis. *Science* **2007**, *317*, 496–499. (d) Faßbach, T. A.; Vorholt, A. J.; Leitner, W. The Telomerization of 1,3-Dienes – A Reaction Grows Up. *ChemCatChem* **2019**, *11*, 1153–1166.

(3) For selected recent examples of transition metal-catalyzed hydroetherification of unactivated alkenes, see: (a) Qian, H.; Han, X.; Widenhoefer, R. A. Platinum-Catalyzed Intramolecular Hydroalkoxylation of γ- and δ-Hydroxy Olefins to Form Cyclic Ethers. *J. Am. Chem. Soc.* **2004**, *126*, 9536–9537. (b) Sevov, C. S.; Hartwig, J. F. Iridium-Catalyzed, Intermolecular Hydroetherification of Unactivated Aliphatic Alkenes with Phenols. *J. Am. Chem. Soc.* **2013**, *135*, 9303–9306. (c) Schlüter, J.; Blazejak, M.; Boeck, F.; Hintermann, L. Asymmetric Hydroalkoxylation of Non-Activated Alkenes: Titanium-Catalyzed Cycloisomerization of Allylphenols at High Temperatures. *Angew. Chem. Int. Ed.* **2015**, *54*, 4014–4017. (d) Marcyk, P. T.; Cook, S. P. Iron-Catalyzed Hydroamination and Hydroetherification of Unactivated Alkenes. *Org. Lett.* **2019**, *21*, 1547–1550.

(4) For selected recent examples of Brønsted acid-catalyzed hydroetherification of unactivated alkenes, see: (a) Coulombel, L.; Duñach, E. Triflic Acid-Catalysed Cyclisation of Unsaturated Alcohols. *Green Chem.* **2004**, *6*, 499–501. (b) Li, Z.; Zhang, J.; Brouwer, C.; Yang, C.-G.; Reich, N. W.; He, C. Brønsted Acid Catalyzed Addition of Phenols, Carboxylic Acids, and Tosylamides to Simple Olefins. *Org. Lett.* **2006**, *8*, 4175–4178. (c) Tsuiji, N.; Kennemur, J. L.; Buyck, T.; Lee, S.; Prévost, S.; Kaib, P. S. J.; Bykov, D.; Farès, C.; List, B. Activation of Olefins via Asymmetric Brønsted Acid Catalysis. *Science* **2018**, *359*, 1501–1505.

(5) For selected recent examples of hydroetherification of unactivated alkenes using other catalyst systems, see: (a) Leger, P. R.; Murphy, R. A.; Pushkarskaya, E.; Sarpong, R. Synthetic Efforts toward the Lycopodium Alkaloids Inspires a Hydrogen Iodide Mediated Method for the Hydroamination and Hydroetherification of Olefins. *Chem. Eur. J.* **2015**, *21*, 4377–4383. (b) Fujita, S.; Abe, M.; Shibuya, M.; Yamamoto, Y. Intramolecular Hydroalkoxylation of Unactivated Alkenes Using Silane–Iodine Catalytic System. *Org. Lett.* **2015**, *17*, 3822–3825. (c) Luo, C.; Bandar, J. S. Superbase-Catalyzed Anti-Markovnikov Alcohol Addition Reactions to Aryl Alkenes. *J. Am. Chem. Soc.* **2018**, *140*, 3547–3550.

(6) (a) Hamilton, D. S.; Nicewicz, D. A. Direct Catalytic Anti-Markovnikov Hydroetherification of Alkenols. *J. Am. Chem. Soc.* **2012**, *134*, 18577–18580. (b) Romero, N.; Nicewicz, D. A. Mechanistic Insight into the Photoredox Catalysis of Anti-Markovnikov Alkene Hydrofunctionalization Reactions. *J. Am. Chem. Soc.* **2014**, *136*, 17024-17035. (c) Margrey, K. A.; Nicewicz, D. A. A General Approach to Catalytic Alkene Anti-Markovnikov Hydrofunctionalization Reactions via Acridinium Photoredox Catalysis. *Acc. Chem. Res.* **2016**, *49*, 1997–2006.

(7) For pioneering reports on alkoxy radical addition to olefins, see: (a) Shelton, J. R.; Uzelmeier, C. W. Reactions of Alkenes with Di-*t*-Butyl Peroxide and *t*-Butyl Peroxypivalate. *J. Org. Chem.* **1970**, *35*, 1576–1581. (b) Elson, I. H.; Mao, S. W.; Kochi, J. K. Electron Spin Resonance Study of Addition of Alkoxy Radicals to Olefins. *J. Am. Chem. Soc.* **1975**, *97*, 335–341. (c) Jones, M. J.; Moad, G.; Rizzardo, E.; Solomon, D. H. The Philicity of *tert*-Butoxy Radicals. What Factors Are Important in Determining the Rate and Regiospecificity of *tert*-Butoxy Radical Addition to Olefins? *J. Org. Chem.* **1989**, *54*, 1607–1611.

(8) For reviews and examples of intramolecular hydroetherification mediated by alkoxy radicals, see: (a) Surzur, J. M.; Bertrand, M. P.; Nouguier, R. Heterocyclisation Radicalaire de Nitrites Ethyleniques. *Tetrahedron Lett.* **1969**, *48*, 4197–4200. (b) Johns, A.; Murphy, J. A. Cyclisations of Allyloxy Radicals. *Tetrahedron Lett.* **1988**, *29*, 837–840. (c) Hartung, J.; Gallou, F. Ring Closure Reactions of Substituted 4-Pentenyl-1-Oxy Radicals. The Stereoselective Synthesis of Functionalized Disubstituted Tetrahydrofurans. *J. Org. Chem.* **1995**, *60*, 6706–6716. (d) Hartung, J. Stereoselective Construction of the Tetrahydrofuran Nucleus by Alkoxyl Radical Cyclizations. *Eur. J. Org. Chem.* **2001**, 619–632. (e) Hartung, J.; Gottwald, T.; Špehar, K. Selectivity in the Chemistry of Oxygen-Centered Radicals – The Formation of Carbon-Oxygen Bonds. *Synthesis* **2002**, *11*, 1469–1498. (f) Hartung, J.; Kneuer, R. Synthesis of Enantiopure (2*R*)-Configured Muscarine Alkaloids *via* Selective Alkoxyl Radical Ring-Closure Reactions. *Tetrahedron: Asymmetry* **2003**, *14*, 3019–3031. (g) Hartung, J.; Kneuer, R.; Rummey, C.; Bringmann, G. On the 6-*endo* Selectivity in 4-Penten-1-Oxyl Radical Cyclizations. *J. Am. Chem. Soc.* **2004**, *126*, 12121–12129. (h) Zlotorzynska, M.; Zhai, H.; Sammis, G. M. Chemoselective Oxygen-Centered Radical Cyclizations onto Silyl Enol Ethers. *Org. Lett.* **2008**, *10*, 5083–5086. (i) Rueda-Becerril, M.; Leung, J. C. T.; Dunbar, C. R.; Sammis, G. M. Alkoxy Radical Cyclizations onto Silyl Enol Ethers Relative to Alkene Cyclization, Hydrogen Atom Transfer, and Fragmentation Reactions. *J. Org. Chem.* **2011**, *76*, 7720–7729. (j) Schur, C.; Kelm, H.; Gottwald, T.; Ludwig, A.; Kneuer, R.; Hartung, J. Annulated and Bridged Tetrahydrofurans from Alkenoxyl Radical Cyclization. *Org. Biomol. Chem.* **2014**, *12*, 8288–8307. (k) Ren, H.; Song, J.-R.; Li, Z.-Y.; Pan, W.-D. Oxazoline-

/Copper-Catalyzed Alkoxyl Radical Generation: Solvent-Switched to Access 3a,3a'-Bisfuroindoline and 3-Alkoxyl Furoindoline. *Org. Lett.* **2019**, *21*, 6774–6778.

(9) For a recent example of intermolecular hydroetherification mediated by alkoxy radicals, see: (a) Barthelemy, A.-L.; Tuccio, B.; Magnier, E.; Dagousset, G. Alkoxyl Radicals Generated under Photoredox Catalysis: A Strategy for Anti-Markovnikov Alkoxylation Reactions. *Angew. Chem. Int. Ed.* **2018**, *57*, 13790–13794. (b) Barthelemy, A.-L.; Tuccio, B.; Magnier, E.; Dagousset, G. Intermolecular Trapping of Alkoxy Radicals with Alkenes: A New Route to Ether Synthesis. *Synlett* **2019**, *30*, 1489-1495.

(10) (a) Yayla, H. G.; Wang, H.; Tarantino, K. T.; Orbe, H. S.; Knowles, R. R. Catalytic Ring-Opening of Cyclic Alcohols Enabled by PCET Activation of Strong O–H Bonds. *J. Am. Chem. Soc.* **2016**, *138*, 10794–10797. (b) Ota, E.; Wang, H.; Frye, N. L.; Knowles, R. R. A Redox Strategy for Light-Driven, Out-of-Equilibrium Isomerizations and Application to Catalytic C–C Bond Cleavage Reactions. *J. Am. Chem. Soc.* **2019**, *141*, 1457–1462. (c) Zhao, K.; Yamashita, K.; Carpenter, J. E.; Sherwood, T. C.; Ewing, W. R.; Cheng, P. T. W.; Knowles, R. R. Catalytic Ring Expansions of Cyclic Alcohols Enabled by Proton-Coupled Electron Transfer. *J. Am. Chem. Soc* **2019**, *141*, 8752–8757. (d) Nguyen, S. T.; Murray, P. R. D.; Knowles, R. R. Light-Driven Depolymerization of Native Lignin Enabled by Proton-Coupled Electron Transfer. *ACS Catal.* **2020**, *10*, 800–805.

(11) For recent advances in the generation of alkoxy radicals using visible light photocatalysis, see: (a) Zhang, J.; Li, Y.; Zhang, F.; Hu, C.; Chen, Y. Generation of Alkoxyl Radicals by Photoredox Catalysis Enables Selective C(sp^3)–H Functionalization under Mild Reaction Conditions. *Angew. Chem. Int. Ed.* **2016**, *55*, 1872–1875. (b) Wang, C.; Harms, K.; Meggers, E. Catalytic Asymmetric C_{sp3}–H Functionalization under Photoredox Conditions by Radical Translocation and Stereocontrolled Alkene Addition. *Angew. Chem. Int. Ed.* **2016**, *55*, 13495–13498. (c) Wu, X.; Wang, M.; Huan, L.; Wang, D.; Wang, J.; Zhu, C. Tertiary-Alcohol-Directed Functionalization of Remote C(sp^3)–H Bonds by Sequential Hydrogen Atom and Heteroaryl Migrations. *Angew. Chem. Int. Ed.* **2018**, *57*, 1640–1644. (d) Hu, A.; Guo, J.-J.; Pan, H.; Tang, H.; Gao, Z.; Zuo, Z. δ-Selective Functionalization of Alkanols Enabled by Visible-Light-Induced Ligand-to-Metal Charge Transfer. *J. Am. Chem. Soc.* **2018**, *140*, 1612–1616. (e) Guo, J.-J.; Hu, A.; Zuo, Z. Photocatalytic Alkoxy Radical-Mediated Transformations. *Tetrahedron Lett.* **2018**, *59*, 2103–2111. (f) Bao, X.; Wang, Q.; Zhu, J. Dual Photoredox/Copper Catalysis for the Remote C(sp^3)–H Functionalization of Alcohols and Alkyl Halides by *N*-Alkoxypyridinium Salts. *Angew. Chem. Int. Ed.* **2019**, *58*, 2139–2143.

(12) For general references on PCET, see: (a) Reece, S. Y.; Nocera, D. G. Proton-Coupled Electron Transfer in Biology: Results from Synergistic Studies in Natural and Model Systems. *Annu. Rev. Biochem.* **2009**, *78*, 673–699. (b) Warren, J. J.; Tronic, T. A.; Mayer, J. M. Thermochemistry of Proton-Coupled Electron Transfer Reagents and Its Implications. *Chem. Rev.* **2010**, *110*, 6961–7001. (c) Weinberg, D. R.; Gagliardi, C. J.; Hull, J. F.; Murphy, C. F.; Kent, C. A.; Westlake, B. C.; Paul, A.; Ess, D. H.; McCafferty, D. G.; Meyer, T. J. Proton-Coupled Electron Transfer. *Chem. Rev.* **2012**, *112*, 4016–4093. (d) Miller, D. C.; Tarantino, K. T.; Knowles, R. R. Proton-Coupled Electron Transfer in Organic Synthesis: Fundamentals, Applications, and Opportunities. *Top. Curr. Chem.* **2016**, *374*, 30. (e) Gentry, E. C.; Knowles, R. R. Synthetic Applications of Proton-Coupled Electron Transfer. *Acc. Chem. Res.* **2016**, *49*, 1546–1556.

(13) Qiu, G.; Knowles, R. R. Understanding Chemoselectivity in Proton-Coupled Electron Transfer: A Kinetic Study of Amide and Thiol Activation. *J. Am. Chem. Soc.* **2019**, *141*, 16574–16578.

(14) Miller, D. C.; Choi, G. J.; Orbe, H. S.; Knowles, R. R. Catalytic Olefin Hydroamidation Enabled by Proton-Coupled Electron Transfer. *J. Am. Chem. Soc.* **2015**, *137*, 13492–13495.

(15) Zhu, Q.; Gentry, E. C.; Knowles, R. R. Catalytic Carbocation Generation Enabled by the Mesolytic Cleavage of Alkoxyamine Radical Cations. *Angew. Chem. Int. Ed.* **2016**, *55*, 9969–9973.

(16) Rueping, M.; Nachtsheim, B. J.; Ieawsuwan, W.; Atodiresei, I. Modulating the Acidity: Highly Acidic Brønsted Acids in Asymmetric Catalysis. *Angew. Chem. Int. Ed.* **2011**, *50*, 6707–6720.

(17) Carvalho, P. J.; Ventura, S. P. M.; Batista, M. L. S.; Schröder, B.; Gonçalves, F.; Esperança, J.; Mutelet, F.; and Coutinho, J. A. P. Understanding the Impact of the Central Atom on the Ionic Liquid Behavior: Phosphonium vs Ammonium Cations. *J. Chem. Phys.* **2014**, *140*, 064505.

(18) For selected reviews and examples of olefin carboetherication, see: (a) Wolfe, J. P.; Rossi, M. A. Stereoselective Synthesis of Tetrahydrofurans via the Palladium-Catalyzed Reaction of Aryl Bromides with γ-Hydroxy Alkenes: Evidence for an Unusual Intramolecular Olefin Insertion into a Pd(Ar)(OR) Intermediate. *J. Am. Chem. Soc.* **2004**, *126*, 1620–1621. (b) Wolfe, J. P. Palladium-Catalyzed Carboetherification and Carboamination Reactions of γ-Hydroxy- and γ-Aminoalkenes for the Synthesis of Tetrahydrofurans and Pyrrolidines. *Eur. J. Org. Chem.* **2007**, 571–582. (c) Zhu, R.; Buchwald, S. L. Combined Oxypalladation/C–H Functionalization: Palladium(II)-Catalyzed Intramolecular Oxidative Oxyarylation of Hydroxyalkenes. *Angew. Chem. Int. Ed.* **2012**, *51*, 1926–1929. (d) Miller, Y.; Miao, L.; Hosseini, A. S.; Chemler, S. R. Copper-Catalyzed Intramolecular Alkene Carboetherification: Synthesis of Fused-Ring and Bridged-Ring Tetrahydrofurans. *J. Am. Chem. Soc.* **2012**, *134*, 12149–12156.

Insert Table of Contents artwork here

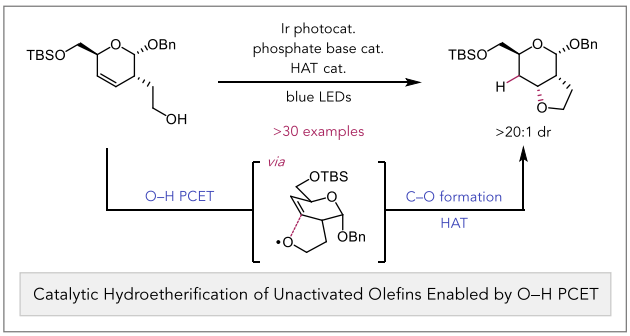

Catalytic Hydroetherification of Unactivated Olefins Enabled by O–H PCET